

Electronic Supplementary Information (ESI)

**Solution-processed white OLEDs with power efficiency over 90 lm W⁻¹
by triplet exciton management with a high triplet energy level
interfacial exciplex host and a high reverse intersystem crossing rate
blue TADF Emitter**

Liang Chen,^{ab} Yufei Chang,^{ab} Song Shi,^{ab} Shumeng Wang^{*a} and Lixiang Wang^{*ab}

^a State Key Laboratory of Polymer Physics and Chemistry, Changchun Institute of Applied Chemistry, Chinese Academy of Sciences, Changchun, 130022, P. R. China

^b School of Applied Chemistry and Engineering, University of Science and Technology of China, Hefei 230026, P. R. China

Corresponding Author

*E-mail: wangshumeng@ciac.ac.cn, lixiang@ciac.ac.cn

The calculation of the reverse intersystem crossing (RISC) rate constant (k_{RISC}):

$$k_r = \frac{\Phi_F}{\tau_p} \quad (1)$$

$$\Phi_{PL} = \frac{k_r}{k_r + k_{IC}} \quad (2)$$

$$\Phi_F = \frac{k_r}{k_r + k_{IC} + k_{ISC}} \quad (3)$$

$$\Phi_{IC} = \frac{k_{IC}}{k_r + k_{IC} + k_{ISC}} \quad (4)$$

$$\Phi_{ISC} = 1 - \Phi_F - \Phi_{IC} = \frac{k_{ISC}}{k_r + k_{IC} + k_{ISC}} \quad (5)$$

$$\Phi_{RISC} = \frac{\Phi_{DF}}{\Phi_{ISC}} \quad (6)$$

$$k_{RISC} = \frac{k_p k_d \Phi_{DF}}{k_{ISC} \Phi_{DF}} \quad (7)$$

$$k_p = \frac{1}{\tau_p}; k_d = \frac{1}{\tau_d} \quad (8)$$

Where k_r , k_{ISC} , k_{RISC} , k_p , and k_d stand for the rate of the radiative decay, the intersystem crossing, the reverse intersystem crossing, the prompt decay, and the delayed decay, respectively, while Φ_{PL} , Φ_F and Φ_{DF} are the photoluminescence quantum yield (PLQY) and the PLQY of the prompt and delayed part, respectively.

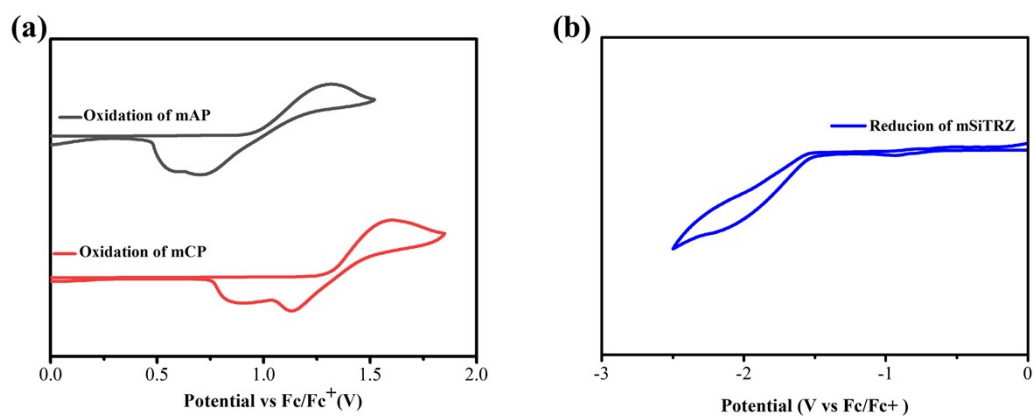


Fig. S1 a) Cyclic voltammetry curves of mAP and mCP. b) Cyclic voltammetry curves of mSiTRZ.

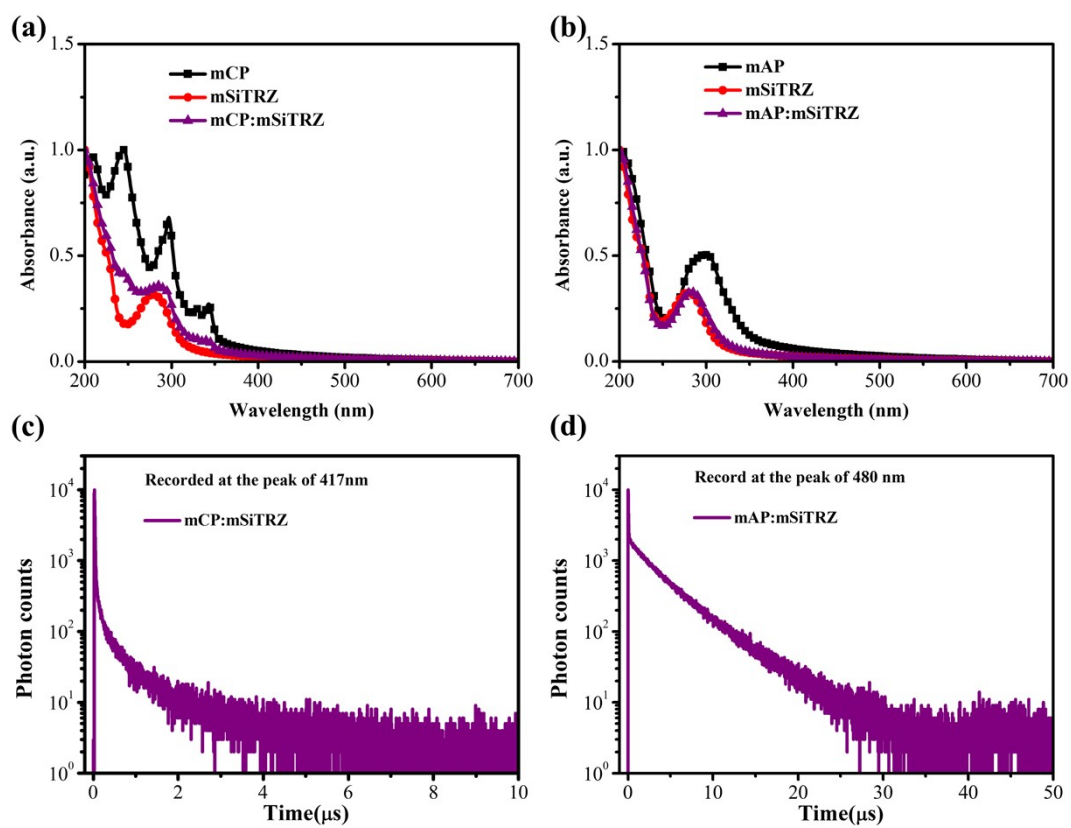


Fig. S2 Optical characteristics of exciplex: a, b) UV-vis absorption spectra of constituent materials and mixed films. c, d) The transient PL spectra of exciplex.

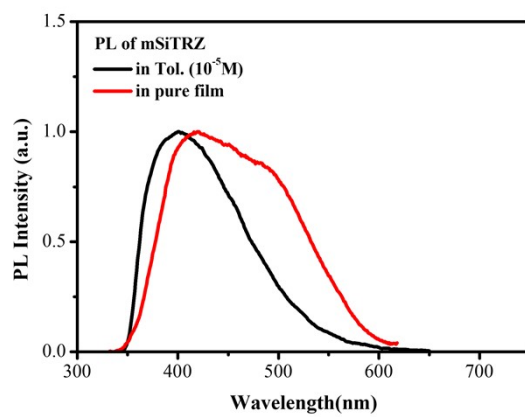


Fig. S3 PL spectra of mSiTRZ in dilute solution and pure film.

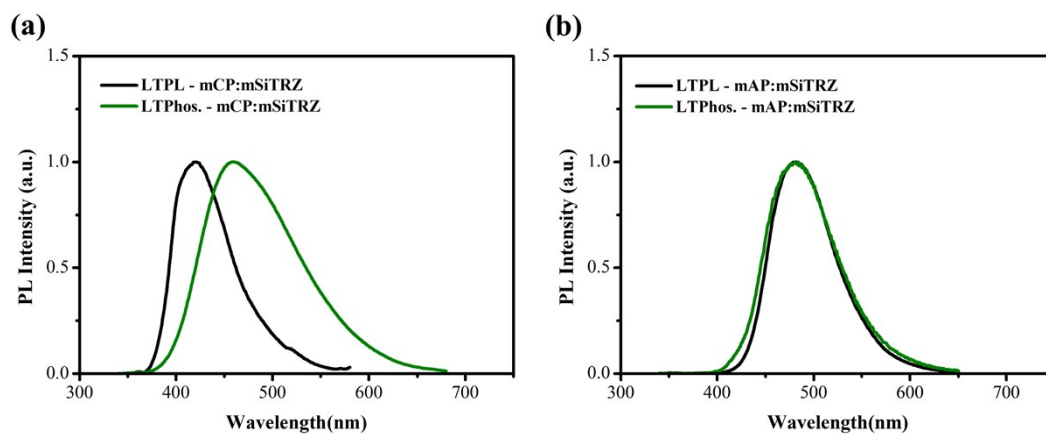


Fig. S4 Low-temperature spectra of exciplex. a) mCP:mSiTRZ. b) mAP:mSiTRZ.

Table S1. Photophysical characteristics of exciplex.

Exciplex	PL ^{a)} [nm]	FWHM ^{a)} [nm]	τ_d ^{b)} [μs]	S₁ ^{c)} [eV]	T₁ ^{d)} [eV]	ΔE_{ST} ^{e)} [eV]
mCP: mSiTRZ	417	66	0.36	3.26	3.15	0.11
mAP: mSiTRZ	480	75	3.58	2.91	2.90	0.01

^{a)}Obtained from the PL spectra of exciplex at 298 K. ^{b)}Average lifetime of delayed component determined from the transient PL spectra. ^{c, d)}Determined from the onset of the PL and phosphorescent spectra at 77 K. ^{e)}Calculated according to the equation: $\Delta E_{ST} = S_1 - T_1$.

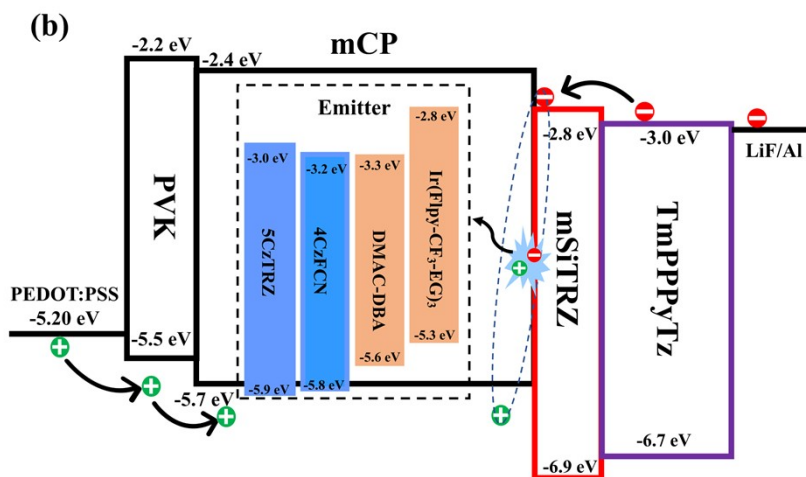
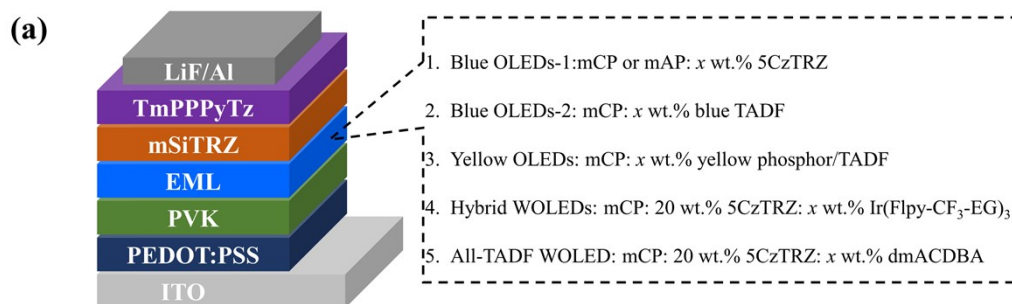


Fig. S5 (a) The device structure used in this work. (b) The energy level diagram of the device

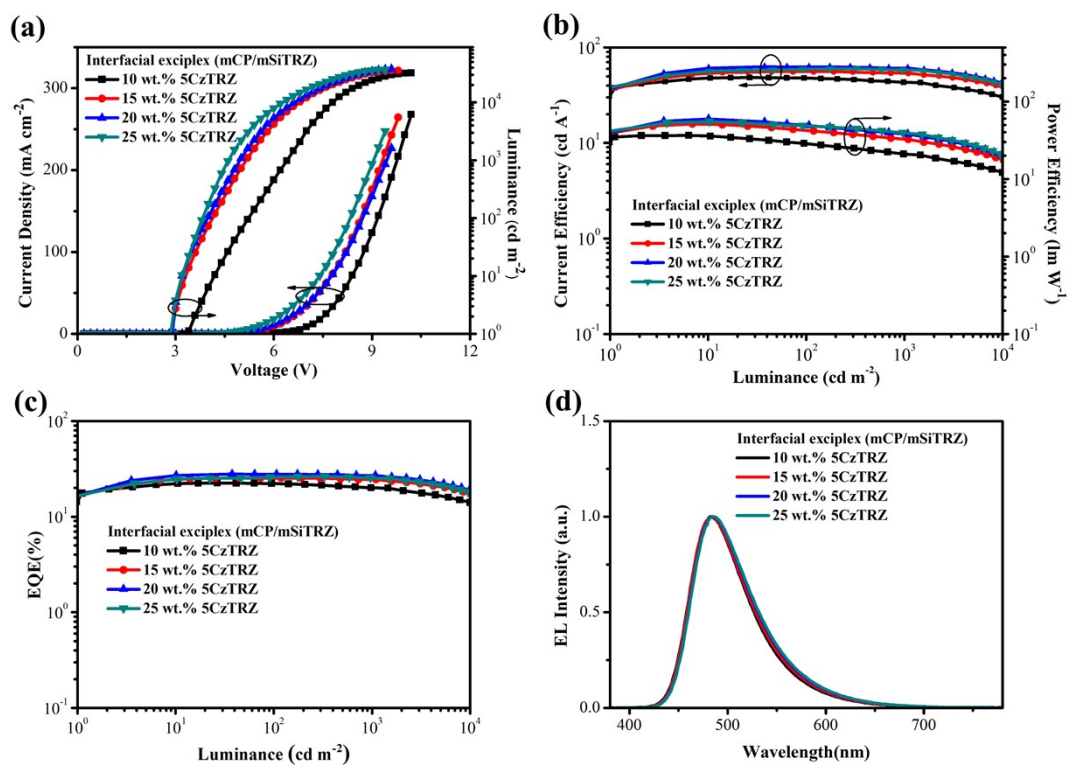


Fig. S6 Performance of solution-processed blue TADF-OLEDs with mCP/mSiTRZ interfacial exciplex host. a) Current density-voltage-luminance characteristics. b) CE-luminance-PE characteristics. c) EQE-luminance characteristics. d) EL spectra at 1000 cd m⁻².

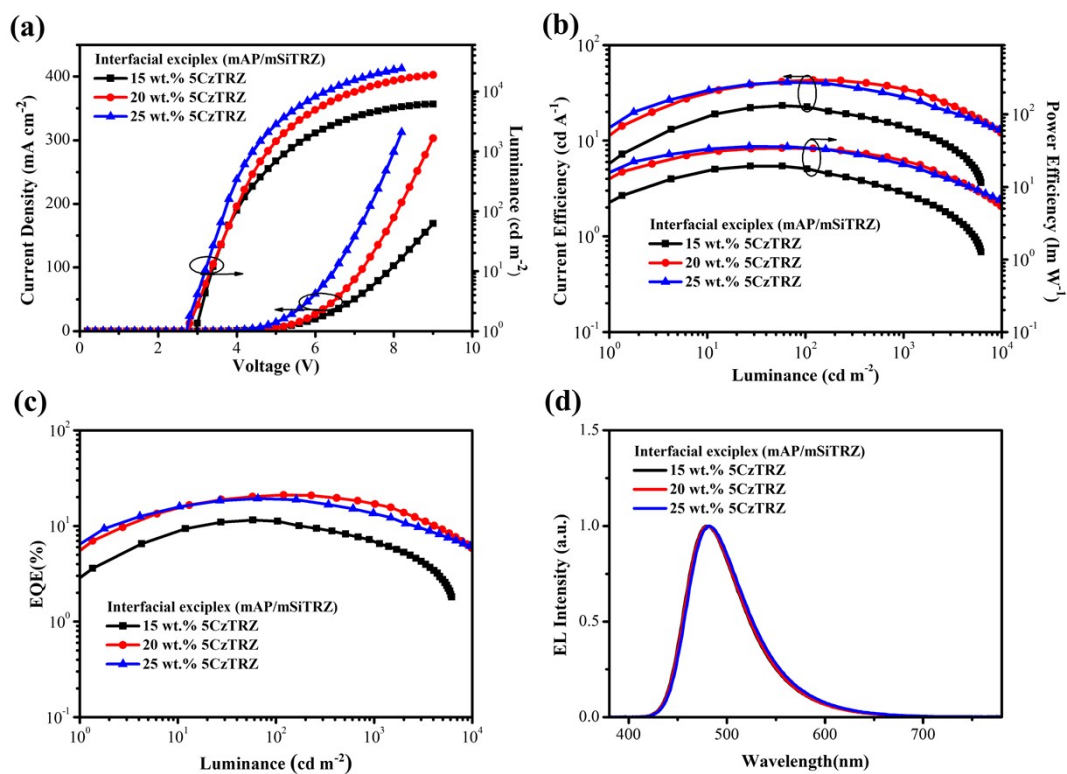


Fig. S7 Performance of solution-processed blue TADF-OLEDs with mAP/mSiTRZ interfacial exciplex host. a) Current density-voltage-luminance characteristics. b) CE-luminance-PE characteristics. c) EQE-luminance characteristics. d) EL spectra at 1000 cd m⁻².

Table S2. Summary of performance for solution-processed blue TADF-OLEDs based on interfacial exciplex host.

Blue device	$V_{on/1000/5000}^a)$ [V]	$CE_{max/1000/5000}^b)$ [cd A ⁻¹]	$PE_{max/1000/5000}^c)$ [lm W ⁻¹]	$EQE_{max/1000/5000}$ [%]	Roll-off _{1000/5000} [%]	CIE (x, y)
mCP/mSiTRZ						
10wt% 5CzTRZ	3.2/6.7/7.3	48.3/42.9/35.4	36.5/21.0/15.3	22.5/20.0/16.5	11.1/26.6	(0.18, 0.35)
15wt% 5CzTRZ	3.0/5.1/6.1	55.8/53.8/45.2	51.2/32.8/23.2	25.5/24.6/20.6	3.5/19.2	(0.18, 0.36)
20wt% 5CzTRZ	2.9/4.9/5.9	62.9/61.2/49.7	62.5/39.2/26.4	28.1/27.3/22.2	2.8/21.0	(0.19, 0.37)
25wt% 5CzTRZ	2.9/4.6/5.6	59.7/58.1/48.5	55.1/39.7/27.4	26.2/25.5/21.4	2.7/18.3	(0.19, 0.38)
mAP/mSiTRZ						
15wt% 5CzTRZ	3.0/5.3/7.8	23.3/13.7/5.5	19.2/8.1/2.2	11.5/6.8/2.7	40.9/75.2	(0.17, 0.31)
20wt% 5CzTRZ	2.8/4.8/6.0	43.0/34.6/18.6	34.2/22.6/9.7	21.1/17.0/9.0	19.4/57.3	(0.17, 0.32)
25wt% 5CzTRZ	2.7/4.4/5.5	40.9/28.6/16.6	35.9/20.4/9.4	19.4/13.5/7.8	30.4/59.8	(0.18, 0.34)

^{a)} Operating voltage at 1/1000/5000 cd m⁻². ^{b)} Current efficiency. ^{c)} Power efficiency.

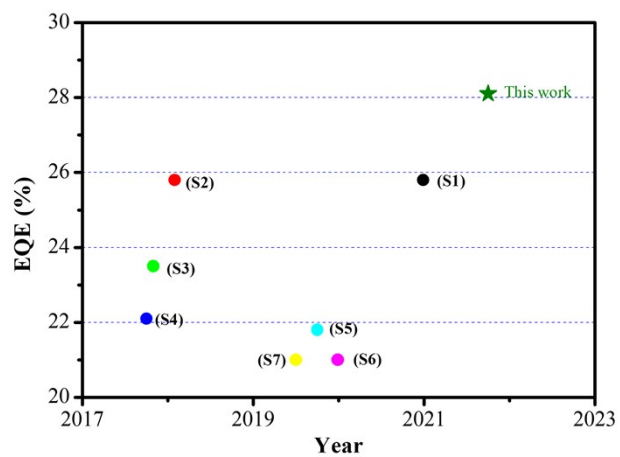


Fig. S8 The EQE-Year of high-performance solution-processed blue TADF-OLEDs reported in the literature.

Table S3. Comparison of the high-performance solution-processed blue TADF-OLEDs reported in the literature.

Host:dopant	V_{on} [V]	PE_{max/1000} [lm W⁻¹]	EQE_{max/1000} [%]	roll-off₁₀₀₀ [%]	CIE₁₀₀₀ (x, y)	Refs
(mCP/mSiTRZ):5CzTRZ	2.9	62.5/39.2	28.1/27.3	2.8	(0.19, 0.37)	This work
2Cz2tCzBn	≈4.3	41.5 /8.3	25.8 /7.1	72.5	(0.21, 0.42)	S1
DPOBBPE:5CzCN	≈5.5	27.1/--	25.8/--	--	(0.17, 0.31)	S2
Cz-3CzCN:Cz-4CzCN	3.5	35.2/--	23.5/7.8	66.8	(0.15, 0.30)	S3
CzSi:MA-TA	≈5.0	--/--	22.1/--	--	(0.15, 0.19)	S4
(mCP/PO-T2T):4CzFCN	3.8	40.9/--	21.8/12.4	43.1	--	S5
DDMACPy:DMAC-TRZ	2.8	44.0/32.3	21.0/18.7	11.0	(0.17, 0.42)	S6
T-CNDF-T- <i>t</i> Cz	6.3	20.8/--	21.0/--	--	(0.19, 0.35)	S7

a) Turn-on voltage at 1 cd m⁻². b) Current efficiency. c) Power efficiency.

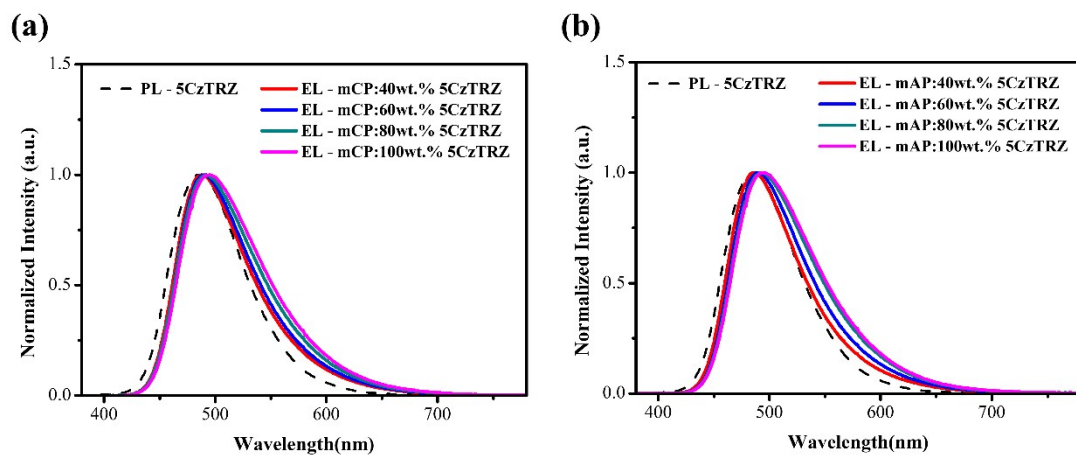


Fig. S9 PL spectrum of 5CzTRZ and EL spectra of solution-processed blue devices at 1000 cd m⁻² with device structure of ITO/PEDOT:PSS/PVK/EML/mSiTRZ/TmPPPyTz/LiF/Al. a) EML= mCP: *x* wt.% 5CzTRZ. b) EML= mAP: *x* wt.% 5CzTRZ.

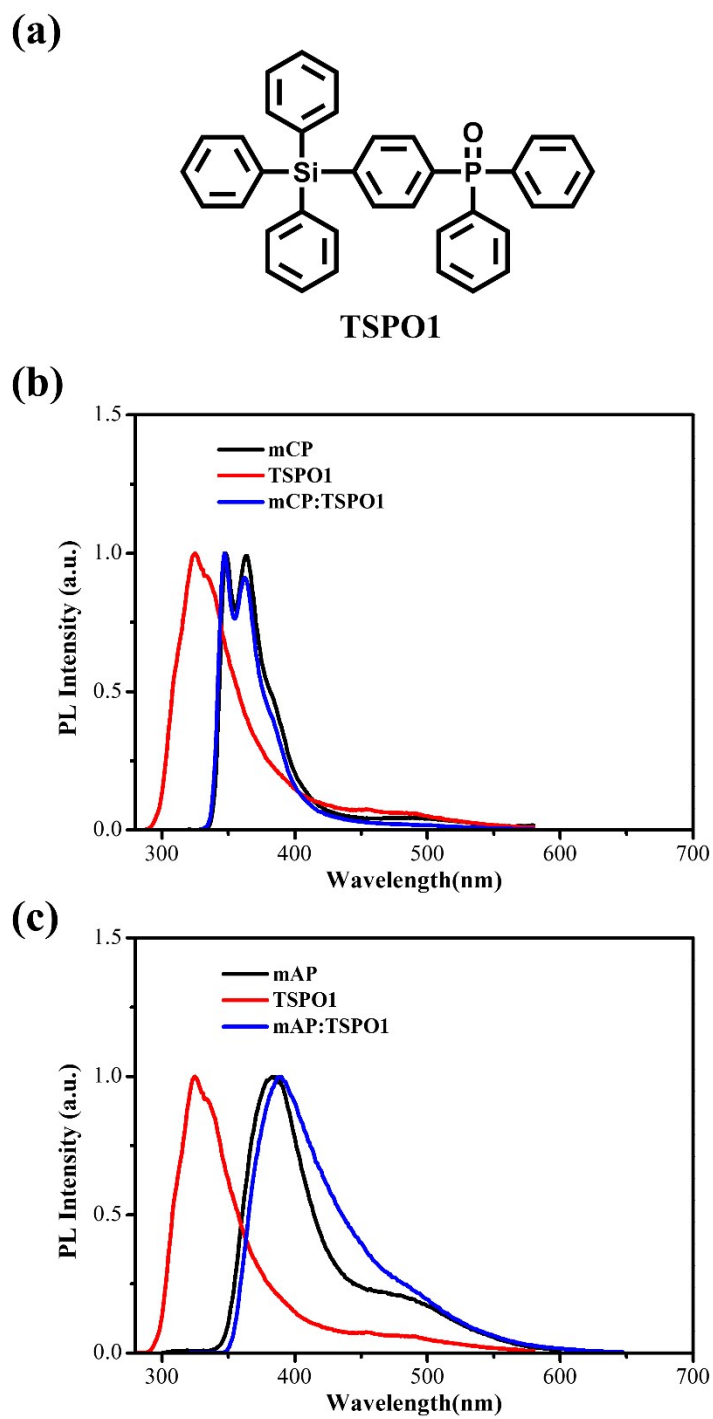


Fig. S10 a) Chemical structure of TSPO1. b) PL spectra of mCP, TSPO1 and mCP:TSPO1 mixed films. c) PL spectra of mAP, TSPO1 and mAP:TSPO1 mixed films.

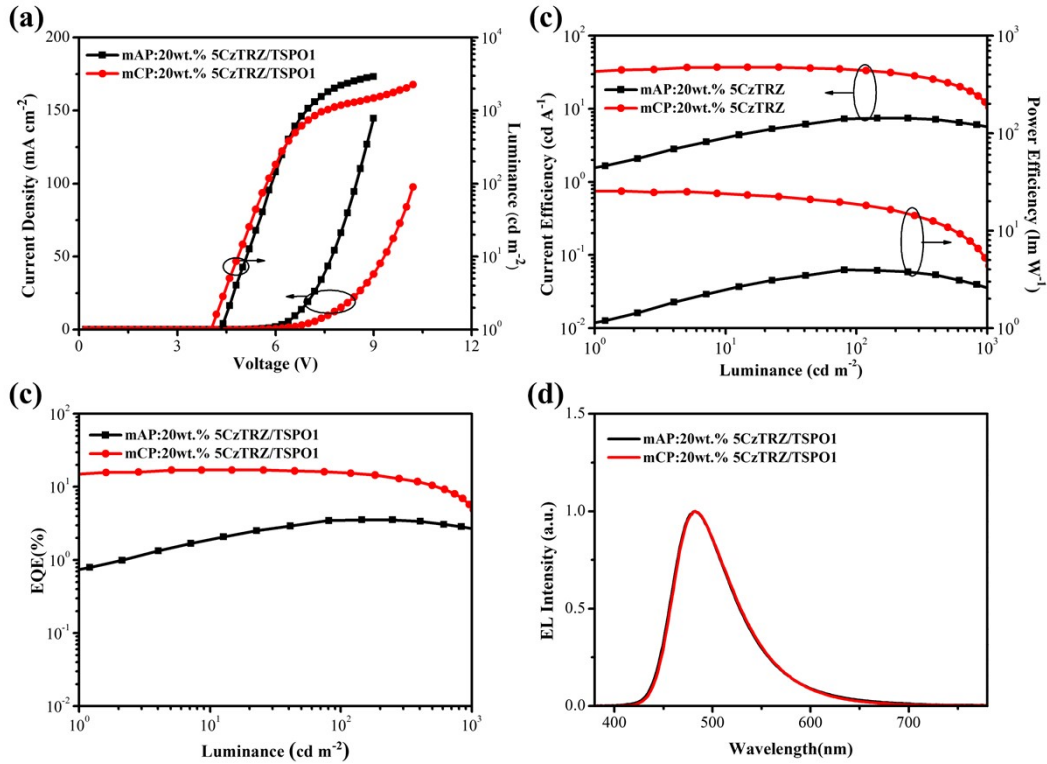


Fig. S11 The solution-processed single-host OLEDs using TSP01 as exciton blocking layer (device structure: ITO/PEDOT:PSS/PVK/ mCP or mAP: 20 wt.% 5CzTRZ/TSP01/TmPPPyTz/LiF/Al). a) Current density-voltage-luminance characteristics. b) CE-luminance-PE characteristics. c) EQE-luminance characteristics. d) EL spectra at 1000 cd m^{-2} .

Table S4. Summary of performance for solution-processed single-host OLEDs using TSPO1 as exciton blocking layer.

Device	V_{on} [V]	Max performance			Device performance at 1000 cd m^{-2}				
		CE ^{b)}	PE ^{c)}	EQE	V_d	CE	PE	EQE	CIE
		[cd A^{-1}]	[lm W^{-1}]	[%]	[V]	[cd A^{-1}]	[lm W^{-1}]	[%]	(x, y)
mCP: 20 wt.% 5CzTRZ/TSPO1	4.2	37.0	25.5	17.1	7.6	10.5	4.4	4.9	(0.19, 0.36)
mAP: 20 wt.% 5CzTRZ/TSPO1	4.3	7.5	4.0	3.5	7.0	5.7	2.5	2.7	(0.18, 0.34)

a) Turn-on voltage at 1 cd m^{-2} . b) Current efficiency. c) Power efficiency.

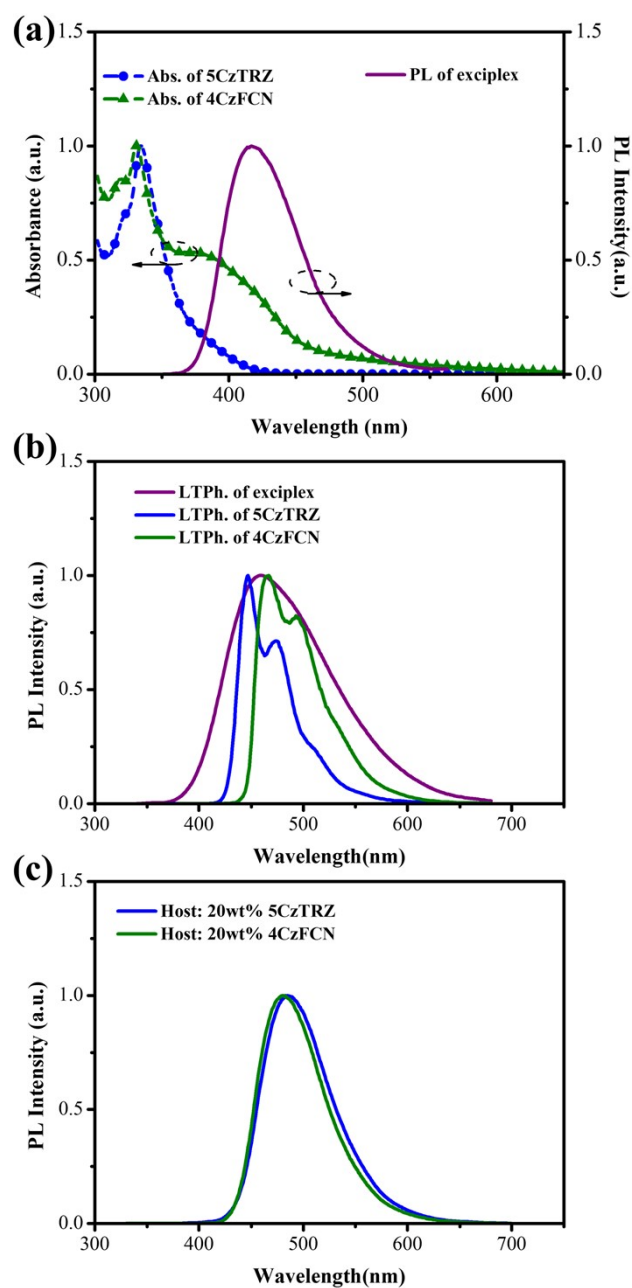


Fig. S12 Optical characteristics of blue emitters. a) UV-vis absorption spectra of 5CzTRZ and 4CzFCN in toluene (10^{-5} M), and PL spectrum of exciplex in film. b) the low-temperature phosphorescence spectra. c) PL spectra in films with 20wt.% blue emitter doped in exciplex (D:A=1:1, by molar ratio).

Table S5. Optical characteristics of 5CzTRZ and 4CzFCN doped film samples.

Film samples [doped in exciplex]	PL ^{a)} [nm]	FWHM ^{a)} [nm]	PLQY ^{b)} [%]	τ_p ^{c)} [ns]	τ_d ^{d)} [μs]	k_{RISC} ^{e)} [s⁻¹]
20 wt.% 5CzTRZ	485	76	96	10.9	2.36	1.15×10^7
20 wt.% 4CzFCN	481	74	83	18.3	12.0	1.31×10^5

^{a)} Obtained from the PL spectra at 298 K. ^{b)} Photoluminescence quantum yield of film samples measured in inert atmosphere. ^{c, d)} Lifetime of the prompt component and delayed component determined from the transient PL spectra. ^{e)} Reverse intersystem crossing rate constant calculated by PLQY and the transient PL spectra.

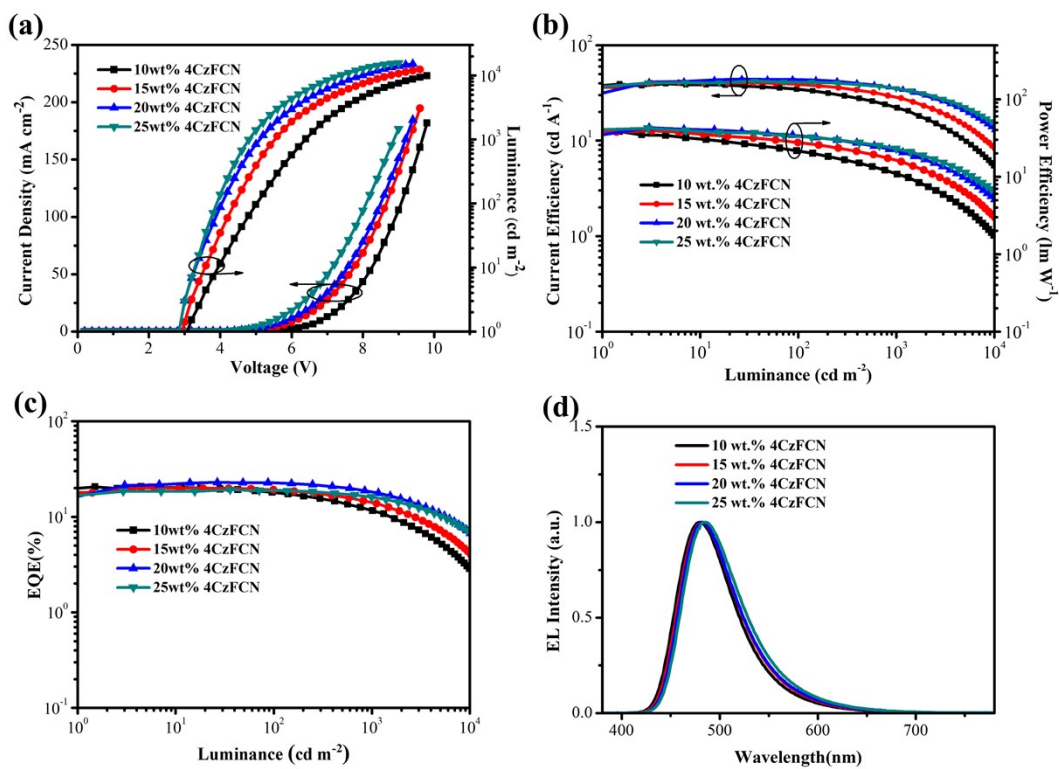


Fig. S13 Performance of solution-processed blue TADF-OLEDs using 4CzFCN as emitter. a) Current density-voltage-luminance characteristics. b) CE-luminance-PE characteristics. c) EQE-luminance characteristics. d) EL spectra at 1000 cd m^{-2} .

Table S6. Summary of performance for solution-processed blue TADF-OLEDs based on mCP/ mSiTRZ interfacial exciplex host.

Blue device	$V_{on/1000/5000}^a)$ [V]	$CE_{max/1000/5000}^b)$ [cd A ⁻¹]	$PE_{max/1000/5000}^c)$ [lm W ⁻¹]	$EQE_{max/1000/5000}$ [%]	$Roll-off_{1000/5000}$ [%]	CIE (x, y)	
10wt.%	4CzFCN	3.1/6.4/8.1	39.4/22.0/10.0	38.3/10.8/3.0	20.7/11.6/5.3	44.0/74.4	(0.16, 0.29)
	5CzTRZ	3.2/6.7/7.3	48.3/42.9/35.4	36.5/21.0/15.3	22.5/20.0/16/.5	11.1/26.6	(0.18, 0.35)
15wt.%	4CzFCN	3.0/5.5/7.2	40.6/28.7/14.6	39.2/16.4/6.4	20.1/14.2/7.2	29.4/64.2	(0.17, 0.32)
	5CzTRZ	3.0/5.1/6.1	55.8/53.8/45.2	51.2/32.8/23.2	25.5/24.6/20.6	3.5/19.2	(0.18, 0.36)
20wt.%	4CzFCN	2.9/5.1/6.7	43.9/35.1/20.2	43.0/21.6/9.5	22.9/18.3/10.6	20.1/53.7	(0.17, 0.33)
	5CzTRZ	2.9/4.9/5.9	62.9/61.2/49.7	62.5/39.2/26.4	28.1/27.3/22.2	2.8/21.0	(0.19, 0.37)
25wt.%	4CzFCN	2.9/4.8/6.2	42.1/35.2/22.1	42.2/23.0/11.2	19.3/16.1/10.1	16.6/47.7	(0.18, 0.36)
	5CzTRZ	2.9/4.6/5.6	59.7/58.1/48.5	55.1/39.7/27.4	26.2/25.5/21.4	2.7/18.3	(0.19, 0.38)

^{a)} Operating voltage at 1/1000/5000 cd m⁻². ^{b)}Current efficiency. ^{c)}Power efficiency.

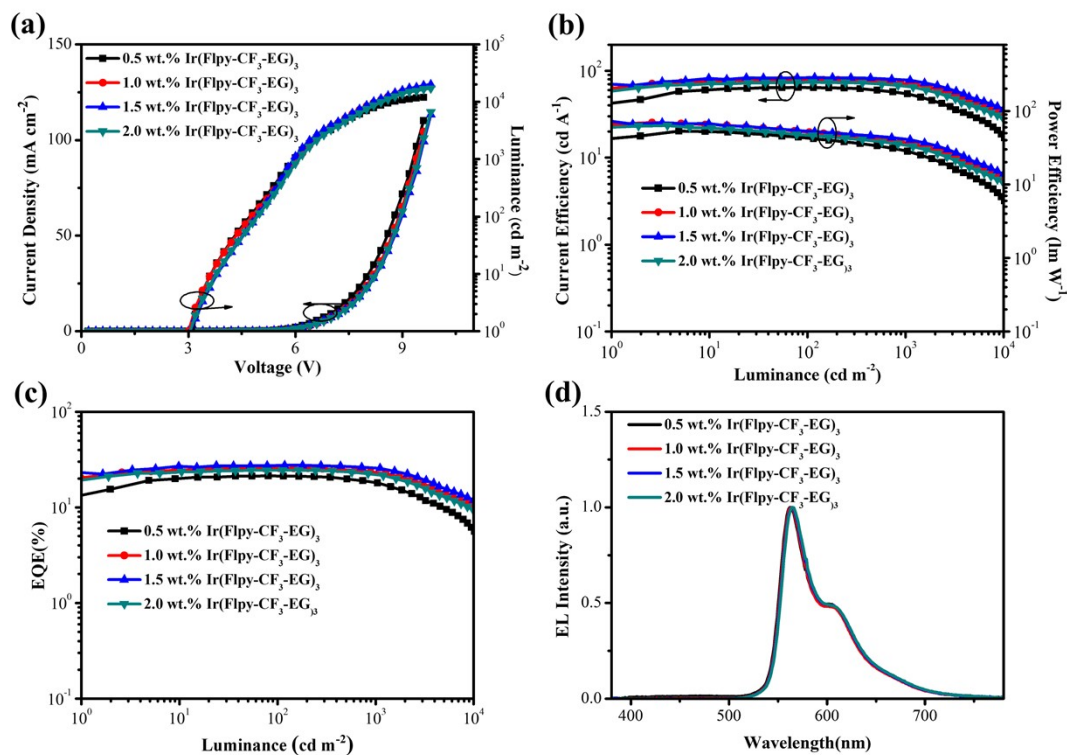


Fig. S14 Performance of solution-processed yellow phosphorescent OLEDs using $\text{Ir}(\text{Flpy-CF}_3\text{-EG})_3$ as emitter. a) Current density-voltage-luminance characteristics. b) CE-luminance-PE characteristics. c) EQE-luminance characteristics. d) EL spectra at 1000 cd m^{-2} .

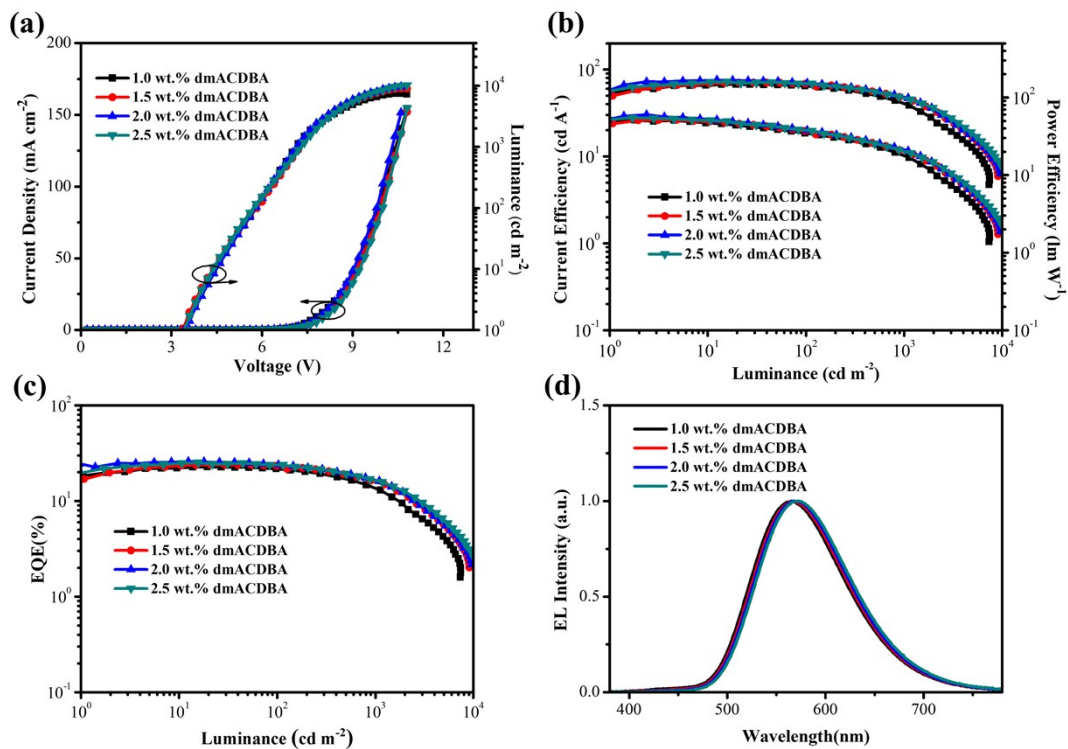


Fig. S15 Performance of solution-processed yellow TADF-OLEDs using dmACDBA as emitter. a) Current density-voltage-luminance characteristics. b) CE-luminance-PE characteristics. c) EQE-luminance characteristics. d) EL spectra at 1000 cd m⁻².

Table S7. Summary of performance for solution-processed yellow OLED devices based on interfacial exciplex host.

Device	$V_{on}^{a)}$ [V]	Max performance			Device performance at 1000 $cd\ m^{-2}$				
		CE ^{b)}	PE ^{c)}	EQE	V_d	CE	PE	EQE	CIE
		[$cd\ A^{-1}$]	[$lm\ W^{-1}$]	[%]	[V]	[$cd\ A^{-1}$]	[$lm\ W^{-1}$]	[%]	(x, y)
0.5 % Ir(Flpy-CF ₃ -EG) ₃	3.1	63.9	53.3	21.2	6.0	54.2	28.4	18.0	(0.50, 0.49)
1.0 % Ir(Flpy-CF ₃ -EG) ₃	3.0	78.7	69.5	25.6	6.0	71.3	39.4	20.3	(0.50, 0.49)
1.5 % Ir(Flpy-CF ₃ -EG) ₃	3.0	83.5	69.2	27.5	6.0	78.0	41.7	25.8	(0.51, 0.49)
2.0 % Ir(Flpy-CF ₃ -EG) ₃	3.0	73.8	63.2	24.5	6.1	66.5	34.2	22.0	(0.51, 0.49)
1.0 % dmACDBA	3.4	67.4	51.2	22.7	7.1	39.6	17.5	13.4	(0.45, 0.52)
1.5 % dmACDBA	3.4	70.8	52.0	24.1	7.2	47.5	20.4	15.6	(0.45, 0.52)
2.0 % dmACDBA	3.4	75.2	59.8	25.8	7.2	47.6	21.4	16.3	(0.46, 0.51)
2.5 % dmACDBA	3.4	72.2	54.7	25.2	7.2	46.0	20.3	16.1	(0.47, 0.51)

a) Turn-on voltage at 1 $cd\ m^{-2}$. b) Current efficiency. c) Power efficiency.

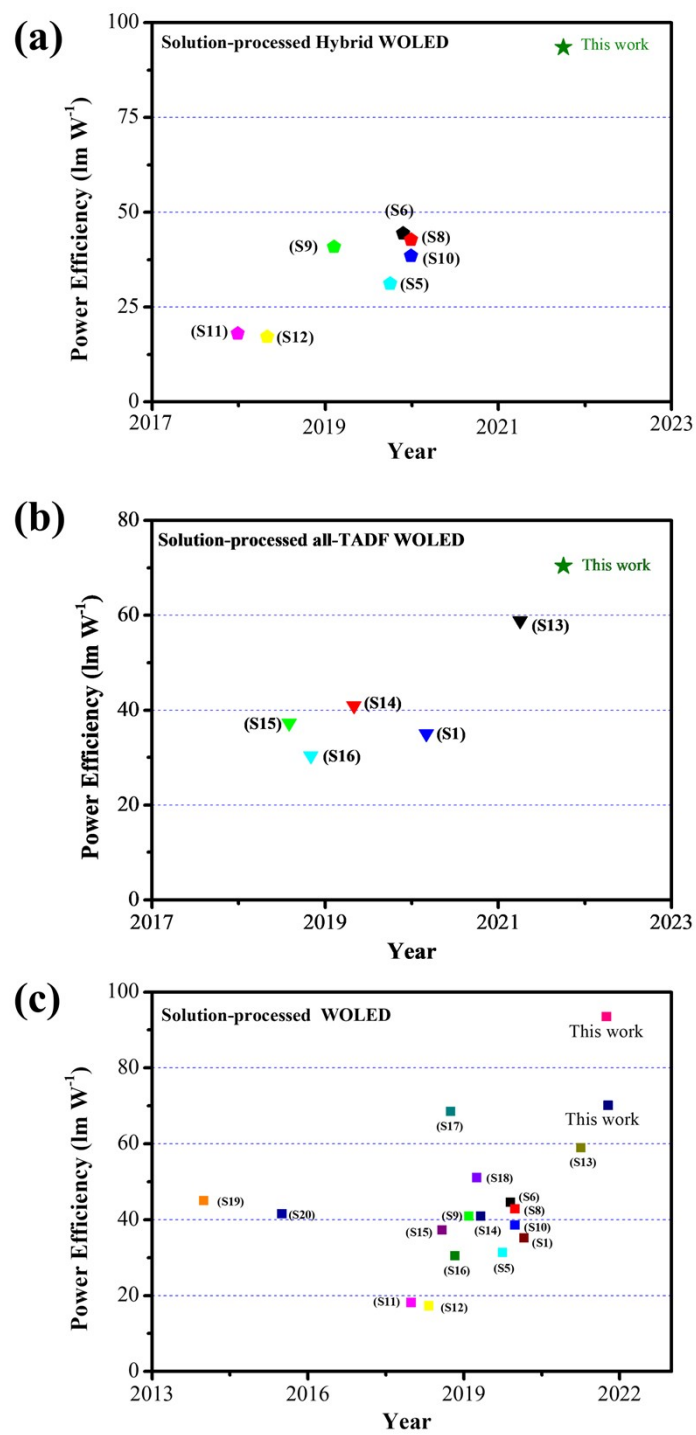


Fig. S16 The PE-Year of high-performance solution-processed WOLEDs reported in the literature.

Table S8. Comparison of the high-performance solution-processed WOLEDs reported in the literature.

Blue emitter		Com. Color	V _{on} [V]	PE _{max/1000} [lm W ⁻¹]	EQE _{max/1000} [%]	CIE (x, y)	Ref.
Hybrid	5CzTRZ	Ir(Flpy-CF ₃ -EG) ₃	2.7	93.5/57.6	31.1/29.7	(0.40, 0.47)	This work
	DMAC-TRZ	Ir(dpm)PQ ₂ and PO-01-TB	2.8	44.5/31.5	17.4/16.2	(0.35, 0.44)	S6
	P-Ir6 (single white-emitting polymers)		3.0	42.8/35.0	17.4/17.1	(0.38, 0.43)	S8
	Cz-OCzBN	PO-01	3.4	40.9/--	17.0/12.0	(0.34, 0.44)	S9
	PCz-4CzCN	PO-01	2.8	38.5/--	18.1/17.8	(0.36, 0.47)	S10
	4CzFCN	Ir(MDQ) ₂ acac	4.1	31.3/--	20.8/11.8	(0.33, 0.39)	S5
	DMAC-TRZ	Ir(dpm)PQ ₂	3.6	18.1/17.0	12.3/--	(0.36, 0.43)	S11
	2CzPN	Ir(MDQ) ₂ (acac).	4.6	17.2/5.2	12.4/4.6	(0.36, 0.41)	S12
All-TADF	5CzTRZ	dmACDBA	3.1	70.4/31.0	27.3/22.8	(0.30, 0.45)	This work
	BD-Cy	YD-TF	2.8	58.9/24.6	20.6/15.1	(0.31, 0.42)	S13
	SDPS-4PhCz	TXO-TPA	3.2	40.9/--	17.6/--	(0.39, 0.44)	S14
	(CDBP:B4PyMPM)	TXO-TPA	3.0	37.3/--	13.4/--	(0.35, 0.39)	S15
	2tCz2CzBn	3DMAC-BP	--	35.1/2.8	27.3/3.5	(0.34, 0.40)	S1
	Cz-3CzCN	Cz-4CzPN	3.9	30.4/9.2	17.3/7.6	(0.34, 0.42)	S16
All-Phos.	Flr- <i>p</i> -OC ₈	Ir(Flpy-CF ₃) ₃	2.8	68.5/47.0	23.6/20.6	(0.43, 0.44)	S17
	B-G2	Ir(Flpy-CF ₃ -EG) ₃	2.7	51.5/23.5	19.3/15.6	(0.36, 0.40)	S18
	Ir(Fppy) ₃	Ir(ppy) ₃ and (Ir(phq) ₃ Ir(ppy) ₂ acac,	3.0	45.0/--	22.0--/	(0.43, 0.43)	S19
	Firpic	Ir(fppq) ₂ acac and Ir(bt) ₂ acac	--	41.8/22.8	16.1/14.7	(0.38, 0.47)	S20

Reference

- [S1] F.-M. Xie, Z.-D. An, M. Xie, Y.-Q. Li, G.-H. Zhang, S.-J. Zou, L. Chen, J.-D. Chen, T. Cheng, J.-X. Tang, *J. Mater. Chem. C* **2020**, *8*, 5769.
- [S2] S. K. Jeon, H.-J. Park, J. Y. Lee, *ACS Appl. Mater. Interfaces* **2018**, *10*, 5700.
- [S3] X. Ban, A. Zhu, T. Zhang, Z. Tong, W. Jiang, Y. Sun, *Chem. Commun.* **2017**, *53*, 11834.
- [S4] Y. Wada, S. Kubo, H. Kaji, *Adv. Mater.* **2018**, *30*, 1705641.
- [S5] Z. He, C. Wang, J. Zhao, X. Du, H. Yang, P. Zhong, C. Zheng, H. Lin, S. Tao, X. Zhang, *J. Mater. Chem. C* **2019**, *7*, 11806.
- [S6] P. S. Ngo, M.-K. Hung, K.-W. Tsai, S. Sharma, S.-A. Chen, *ACS Appl. Mater. Interfaces* **2019**, *11*, 45939.
- [S7] X. Zheng, R. Huang, C. Zhong, G. Xie, W. Ning, M. Huang, F. Ni, F. B. Dias, C. Yang, *Adv. Sci.* **2020**, *7*, 1902087.
- [S8] J. Hu, Q. Li, S. Shao, L. Wang, X. Jing, F. Wang, *Adv. Opt. Mater.* **2020**, *8*, 1902100.
- [S9] X. Ban, F. Chen, Y. Liu, J. Pan, A. Zhu, W. Jiang, Y. Sun, *Chem. Sci.* **2019**, *10*, 3054.
- [S10] X. Ban, Y. Liu, J. Pan, F. Chen, A. Zhu, W. Jiang, Y. Sun, Y. Dong, *ACS Appl. Mater. Interfaces* **2020**, *12*, 1190.
- [S11] J. Y. Wu, S. A. Chen, *ACS Appl. Mater. Interfaces* **2018**, *10*, 4851.
- [S12] W. Li, J. Zhao, L. Li, X. Du, C. Fan, C. Zheng, S. Tao, *Org. Electron.* **2018**, *58*, 276.
- [S13] X. Wang, J. Hu, J. Lv, Q. Yang, H. Tian, S. Shao, L. Wang, X. Jing, F. Wang, *Angew. Chem. Int. Ed.* **2021**, *60*, 2.
- [S14] R. Wang, Y. Liu, T. Hu, X. Wei, J. Liu, Z. Li, X. Hu, Y. Yi, P. Wang, Y. Wang, *Org. Electron.* **2019**, *71*, 24.
- [S15] Y. Liu, X. Wei, Z. Li, J. Liu, R. Wang, X. Hu, P. Wang, T. Qi, Y. Wang, *Adv. Opt. Mater.* **2018**, *6*, 1800978.
- [S16] X. Ban, F. Chen, Y. Zhao, A. Zhu, Z. Tong, W. Jiang, Y. Sun, *ACS Appl. Mater. Interfaces* **2018**, *10*, 37335.

- [S17] S. Wang, L. Zhao, B. Zhang, J. Ding, Z. Xie, L. Wang, W.-Y. Wong, *Iscience* 2018, **6**, 128.
- [S18] S. Wang, Z. Yan, J. Ding, L. Wang, *Adv. Mater. Technol.* **2019**, *4*, 1900137.
- [S19] N. Aizawa, Y. J. Pu, M. Watanabe, T. Chiba, K. Ideta, N. Toyota, M. Igarashi, Y. Suzuri, H. Sasabe, J. Kido, *Nat. Commun.* **2014**, *5*, 5756.
- [S20] S. Wang, B. Zhang, X. Wang, J. Ding, Z. Xie, L. Wang, *Adv. Opt. Mater.* **2015**, *3*, 1349.